Photophysical properties of Cerulean and Venus fluorescent proteins

Pabak Sarkar
University of North Texas Health Science Center
Center for Commercialization of Fluorescent Technologies
3500 Camp Bowie Boulevard
Fort Worth, Texas 76107
and
University of North Texas Health Science Center
Department of Molecular Biology and Immunology
3500 Camp Bowie Boulevard
Fort Worth, Texas 76107

Srinagesh V. Koushik
Steven S. Vogel
National Institutes of Health
National Institute on Alcohol Abuse and Alcoholism
Laboratory of Molecular Physiology
5625 Fishers Lane
Rockville, Maryland 20892

Ignacy Gryczynski
University of North Texas Health Science Center
Center for Commercialization of Fluorescent Technologies
3500 Camp Bowie Boulevard
Fort Worth, Texas 76107
and
University of North Texas Health Science Center
Department of Cell Biology and Genetics
3500 Camp Bowie Boulevard
Fort Worth, Texas 76107

Zygmunt Gryczynski
University of North Texas Health Science Center
Center for Commercialization of Fluorescent Technologies
3500 Camp Bowie Boulevard
Fort Worth, Texas 76107
and
University of North Texas Health Science Center
Department of Molecular Biology and Immunology
3500 Camp Bowie Boulevard
Fort Worth, Texas 76107

Abstract. Cerulean and Venus are recently developed fluorescent proteins, often used as a donor-acceptor pair by researchers in Förster resonance energy transfer–based colocalization studies. We characterized the fluorescent properties of these two proteins in a broad spectral range (form ultraviolet to visible region). Excitation spectra, lifetimes, and polarization spectra show significant energy transfer from aromatic amino acids to the fluorescent protein chromophore. High steady-state anisotropy values and the lack of a fast component in anisotropy decays show that the fluorescent protein chromophore is rigidly fixed within the protein structure. Furthermore, we show that the chromophores are not accessible to external quenchers, such as acrylamide or potassium iodide (KI), allowing the removal of "unwanted" background in the environment with external quencher, while leaving the Cerulean/Venus fluorescence unchanged. [DOI: 10.1117/1.3156842]

Keywords: Förster resonance energy transfer; fluorescence timeline; fluorescence anisotropy.

Paper 08429R received Dec. 8, 2008; revised manuscript received Apr. 14, 2009; accepted for publication May 7, 2009; published online Jun. 24, 2009.

1 Introduction

The use of green fluorescent protein (GFP) as a marker to visualize specific proteins inside living cells has revolutionized cell biology.[1,2] The genetic sequence-encoding GFP has been optimized to facilitate both its expression in mammalian cells,[3,4] as well as its photophysics for best use in elucidating the distribution and intracellular trafficking of genetically tagged proteins.[5–9] The advent of spectral variants of GFP has extended the utility of this technology by enabling the detection of protein-protein interactions *in vivo*. Specific proteins can now be tagged with florescent proteins (FPs) that fluoresce in the blue, green, yellow, orange, or red region.[10] In conjunction with basic light microscopy, many molecular interactions can be implied based on simple colocalization studies.[11] This colocalization approach is however limited by the resolution of light microscopy (typically, 0.2 μm). More sophisticated imaging technologies, including spectral imaging,[12] fluorescence lifetime imaging (FLIM),[13–15] and imaging based on changes in fluorescence anisotropy,[16,17] are being applied to detect interactions between FP-tagged proteins at a resolution of 1–10 nm. One such approach is to monitor Förster resonance energy transfer (FRET) between a protein tagged with a donor-FP and a putative binding partner labeled with an acceptor FP. FRET efficiency can be measured by monitoring reciprocal change in the intensity of

Address all correspondence to Zygmunt Gryczynski, Department of Molecular Biology and Immunology, University of North Texas, 3500 Camp Bowie Blvd, Fort Worth, TX 76107; Tel: 817 735 5471; Fax: 817 735 2118; E-mail: zgryczyn@hsc.unt.edu

1083-3668/2009/14(3)/034047/9/$25.00 © 2009 SPIE

emission from donor and acceptor fluorophores. More advanced and precise measurement of FRET efficiencies can be achieved by monitoring the change of fluorescence lifetime of the donor fluorophore. A high transfer efficiency is often interpreted as an indication of close proximity (<10 nm). Another approach, also based on FRET, is emerging as a method for dynamically monitoring the multimeric state of protein assemblies.[17–19] In this method, fluorescence anisotropy is used to measure energy migration between proteins labeled with the same FP. High anisotropy is indicative of low FRET and vice versa. Furthermore, the amplitude of a drop in anisotropy encodes information on the number of fluorophores in a molecular complex that are participating in the energy migration.

The accurate interpretation of biological FRET experiments utilizing complex quantitative imaging modalities, such as anisotropy analysis or FLIM, relies on an in-depth knowledge of the photophysics of the fluorophores being used. Specifically, for FLIM, it is important to know the lifetime of a fluorophore in the absence of acceptors, and it is also essential to appreciate any other factors that might alter its fluorescence lifetime in the course of an experiment.[20–22] For anisotropy analysis, it is important to know the fundamental anisotropy of a fluorophore (primarily a function of the orientation of its absorption and emission dipoles), how rigidly the fluorophore is attached to a protein of interest and it is also useful to understand any other factors that might alter the orientation of its emission relative to its excitation.[20–22] Furthermore, these sophisticated types of imaging experiments are often difficult to interpret if other endogenous fluorophores are present. Under these circumstances, measured fluorescence lifetimes or anisotropies will be a function of both the fluorophores of interest, as well as the contaminating fluorophores. Unfortunately contaminating fluorophores, like flavins, nicotinamides, porphyrins, etc., are almost always present in living biological samples.

Two of the most popular spectral variant of GFP used for biological FRET studies are Cerulean,[23] a blue emitting FP, and Venus,[24] a yellow emitter. The crystal structure of both of these proteins have been reported.[25,26] Although the photophysics of GFP has been extensively studied,[27–30] this knowledge base may not universally apply to these spectral variants. Furthermore, it has long been suggested that in the FP family FRET might occur between an internal tryptophan and the FP fluorophore.[31–33] If true, this could significantly alter fluorescent protein lifetime and anisotropy in a wavelength-dependent manner, and potentially complicate the interpretation of FRET between Cerulean and Venus. In this study, we characterize the lifetime and anisotropy of purified Cerulean and Venus and in so doing reveal: (*i*) Cerulean and to a lesser extent Venus fluorescence both decay as a double exponential, (*ii*) These fluorophores are rigidly fixed within their beta-barrel structure, and (*iii*) they both express efficient energy transfer between an internal tryptophan and their fluorophores upon UV excitation. Because the fluorophore within Cerulean and Venus are sequestered from the solvent/media due to their protein structure, we find they are resistant to dynamic quenching. We demonstrate how this can be exploited to remove the effects of endogenous fluorophores in these types of FRET experiments.

2 Materials and Methods

Tris buffer (Trizma), Acrylamide (electrophoresis grade), flavin mononucleotide (FMN), and KI were from Sigma-Aldrich Inc., St. Louis, Missouri. 20X PBS, pH-7.5 was from AMRESCO®, Solon, Ohio. The water used for the analysis was deionized (from Millipore® deionizer unit). Both Cerulean and Venus were diluted in 0.1 M Tris, pH 8.5. In the iodide quenching studies with FMN PBS pH 7.5 was used as the buffer as fluorescence of FMN is sensitive to alkaline pH.

2.1 *Purification of Cerulean and Venus*

2.1.1 *Expression and purification of Cerulean and Venus proteins*

6x His-tagged Cerulean and Venus cloned into pRSET B (Invitrogen) and the recombinant proteins were expressed in BL21 (DE3) pLysS bacteria (Invitrogen). Bacteria were lysed, and proteins were purified using Ni-NTA Magnetic Agarose beads (Qiagen), according to the manufacturer's instructions. The protein was concentrated by centrifugation using Centricon centrifugal filter devices (Millipore).

To assess protein integrity and purity of samples 1.4 and 0.14 mg of purified Cerulean and Venus were run on a 10% SDS PAGE gel (Bio-Rad) and Coomassie stained. For the Western blots, 25 ng of Cerulean and Venus proteins were separated on a 10% SDS-PAGE gel under denaturing conditions. The proteins in the gel were transferred onto a polyvinylidine flouride (PVDF) membrane (Immobilon P, Millipore) by electrophoresis. The blot was blocked in a solution containing phosphate-buffered saline (pH 7.4, Invitrogen), 0.05% Tween 20 (Sigma) (PBST), and 5% BSA (ICN Biochemicals) for 30 min. The blot was probed with rabbit anti-GFP polyclonal antibody (ab6556, Abcam; 1:1000 dilution) in PBST and 5% BSA for 1 h at room temperature. The blot was washed in PBST and then probed with a mixture of a goat anti-rabbit HRP conjugated antibody (Pierce, 1:5000 dilution) and HRP-Conjugated Biotin antibody (Cell Signaling, 1:5000 dilution; for biotinlyated mass ladder) in PBST for 30 min. The blot was rinsed and washed as described earlier. Protein bands were visualized by chemiluminescence (SuperSignal West Dura Extended Duration Substrate Kit, Pierce) using a Kodak Image Station 4000R. Densitometry analysis of the protein bands were performed using the analysis software in Kodak Image Station 4000R.

2.2 *Fluorescence Studies*

Varian Cary Eclipse fluorescence spectrophotometer (Varian Inc.) was used for steady-state fluorescence measurements. We used broad range (UV-Visual) polarizers (Manual Polarizer Accessory, Varian Inc., Australia) for measurements in both the visible and ultraviolet regions. At 285 nm, the polarization was $>90\%$, whereas in visible region the polarization was $>96\%$. The mathematical expression used to calculate anisotropy was

$$r = \frac{I_{VV} - GI_{VH}}{I_{VV} + 2GI_{VH}}, \tag{1}$$

where I_{VV} and I_{VH} are vertically excited–vertically emitted and vertically excited–horizontally emitted fluorescence components of the proteins and G is the instrumental G factor.[21]

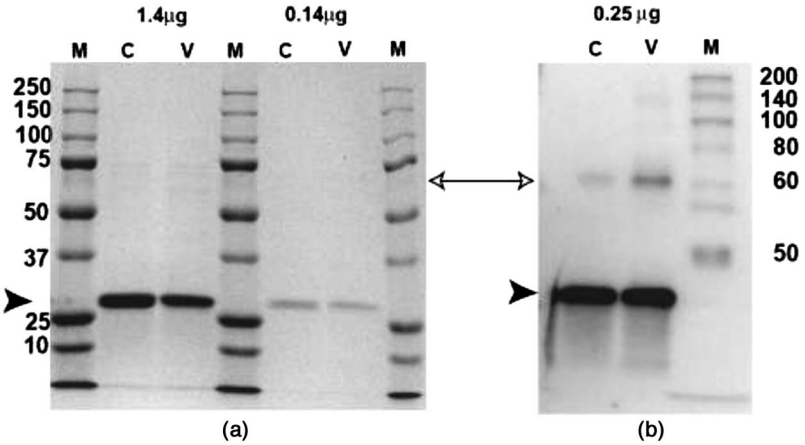

Fig. 1 Characterization of purified proteins. (a) Coomassie staining of a SDS PAGE gel shows 27 kDa (arrow heads) Cerulean (C) and Venus (V) protein bands. There seems to be minor contaminating bands at 60 KDa (double-headed arrow). (b) Western blot of Cerulean and Venus protein, where the Anti GFP antibody strongly cross reacts with the 27 kDa protein.

Time-resolved fluorescence measurements were carried out on FluoTime200 fluorometer (PicoQuant GmbH). This fluorometer is equipped with an ultrafast microchannel plate and is capable to well resolve subnanosecond decays. For studies in the UV region, the samples were excited with a picosecond-pulsed LED light source PLS-280, with bandwidth of 20 nm, manufactured by PicoQuant GmBh. Full width at half maxima (FWHM) of the pulse was ~500 ps, and the repetition rate used for the measurements using the LED was 5 MHz. For visible region studies, 405 nm (for Cerulean) or 470 nm (for Venus) pulsed laser diodes LDH-PC-405 or LDH-PC-470 (PicoQuant GmBh) were used, respectively, in the low-power regime (<70 ps FWHM) with 5 MHz repetition rates. The laser diodes are routinely used to measure fluorescence decays and lifetimes within ±10 ps accuracy. The lifetime data were analyzed by FluoTime software, version 4.0 (PicoQuant GmbH).

For lifetime measurements, a monochromator supported by long wave pass filter on the observation path was used. All the measurements for lifetime decay were performed using magic angle conditions. The decay was fitted with a multiexponential model using the expression

$$I(t) = \sum_i \alpha_i e^{-t/\tau_i}, \tag{2}$$

where $I(t)$ is the intensity at a time t, α_i is the amplitude of i'th component and τ_i is the lifetime of the i'th component.

Time-resolved anisotropy decays were fitted to the multiexponential model using the expression

$$r(t) = \sum r_i e^{(-t/\theta_i)}, \tag{3}$$

where, $r(t)$ is the anisotropy in time t, r_i is the amplitude of the i'th component and θ_i is the correlation time of the i'th component.

All the studies were carried out in room temperature (22°C). The background from the buffer was <1% of the signal, and the background from external quencher KI in buffer was subtracted from all the concerned measurements.

3 Results and Discussion

The purity of Cerulean and Venus were accessed using Coomasie staining of the proteins and Western blot analysis (Fig. 1). The serial dilution of Cerulean and Venus (1.4 and 0.14 mg) reveals a strong band at 27 kDa (FP, arrowheads in Fig 1) and some minor contaminants (double-headed arrows, Fig 1). Densitometry analysis of the Coomassie staining [Fig. 1(a)] revealed that Cerulean was 97% pure and Venus was 90% pure.

3.1 *Steady-State Fluorescence*

Cerulean–Venus is an excellent donor acceptor pair, with selective donor excitation using the 405 or 442-nm laser lines, and observation at 470 nm (no signal from acceptor at this wavelength). This significantly simplifies the FRET measurements and its interpretation. The excitation and emission spectra of both proteins are presented in Fig. 2. There is a significant increase in the excitation intensity in the UV region, at <300 nm. Emission spectra did not change with excitation (data not shown), suggesting either an electronic transition in the chromophore or that excitation energy absorbed by other moieties (such as aromatic amino acids) are efficiently transferred to the chromophore.

To study these possibilities further, we measured polarization spectra. Figure 3 shows steady-state excitation and emission polarization spectra of Cereluan, while Fig. 4 shows the same for Venus protein. Whereas the anisotropy values remain relatively constant within the emission spectra (b), the excitation anisotropies decrease significantly in shorter wavelengths (top panels). Such polarization dependences are common in (*i*) single fluorophore with different excited-state dipoles at higher electronic transition and (*ii*) a donor-acceptor system when excitation anisotropy is observed at acceptor emission. In fact, single-step energy transfer significantly affects anisotropy.

3.2 *Time-Resolved Fluorescence*

Next, we measured fluorescence lifetimes of fluorescent proteins with UV excitation (285 nm) and with direct long-

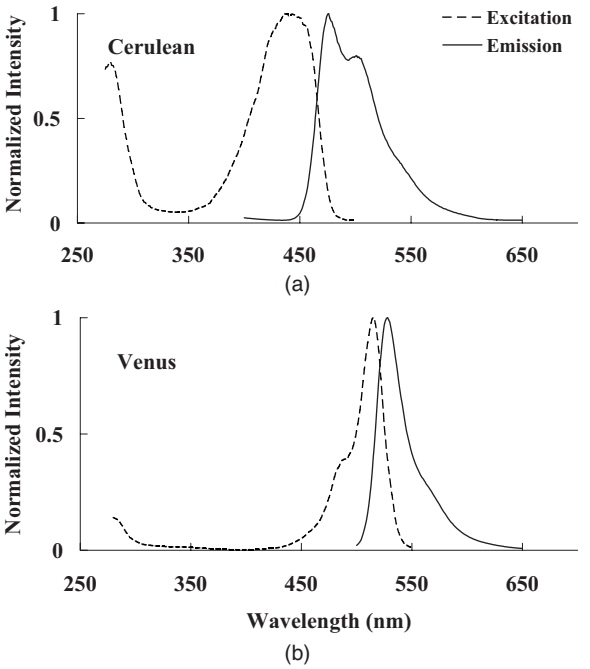

Fig. 2 Excitation and emission spectrum of (a) Cerulean and (b) Venus fluorescent proteins. Fluorescent protein excitation intensity in the UV (280 nm) is thought to be due to FRET from aromatic amino acids to the fluorescent protein chromophore.

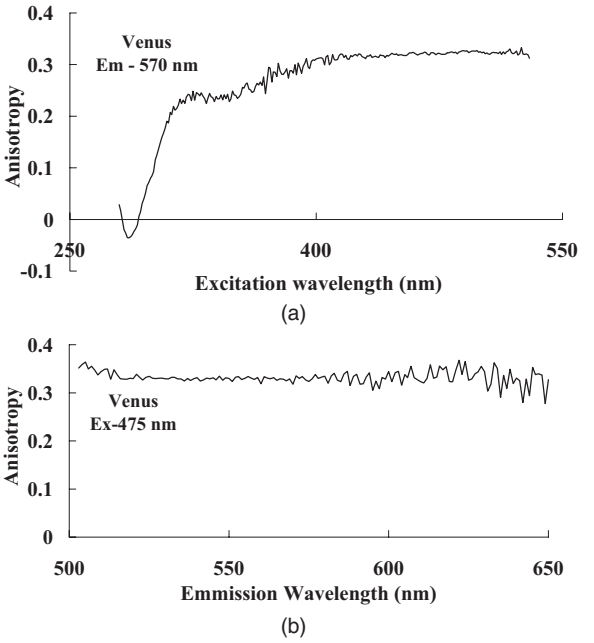

Fig. 4 (a) Excitation and (b) emission steady-state anisotropy of Venus. The high value of steady-state emission anisotropy (b) suggests limited flexibility of the chromophore within the barrel structure of the protein. The negative value of excitation anisotropy in the UV region is consistent with FRET occurring between aromatic amino acids and the fluorescent protein chromophore.

wavelength excitation at 405 and 470 nm for Cerulean and Venus, respectively. The intensity decays of Cereluan and Venus fluorescent proteins with long-wavelength excitation, measured by time-correlated single-photon counting, are presented in Figs. 5 and 6, respectively. One- and two-exponential fits to the experimental data are presented in Table 1. For both proteins, the fluorescence intensity decays were best fitted using a two-exponent decay model, though single exponential fits with lifetimes of 3.18 and 3.03 ns for Cereluan and Venus may in many cases be acceptable. Lifetimes were significantly longer with UV excitation. Furthermore, strong negative lifetime components of ~0.2 ns were

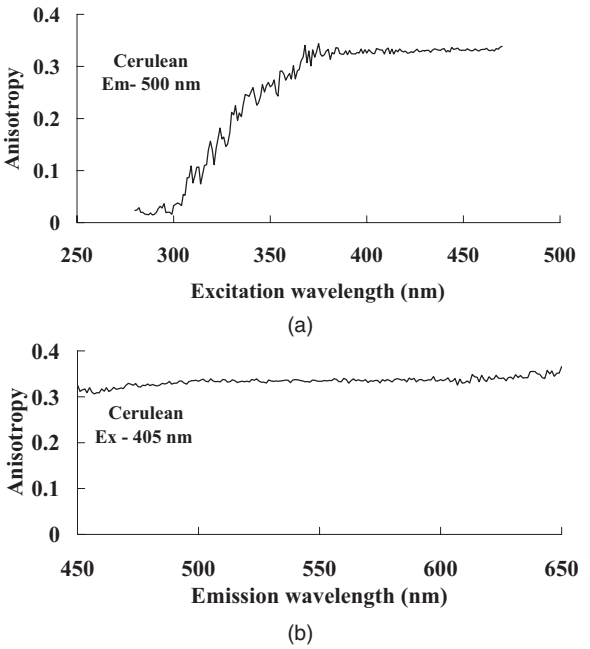

Fig. 3 (a) Excitation and (b) emission steady-state anisotropies of Cerulean. The high value of emission anisotropy, >0.3, suggests limited flexibility of the fluorophore within the protein structure. The rapid decrease of the excitation anisotropy is consistent with FRET between aromatic amino acids and the fluorescent protein chromophore.

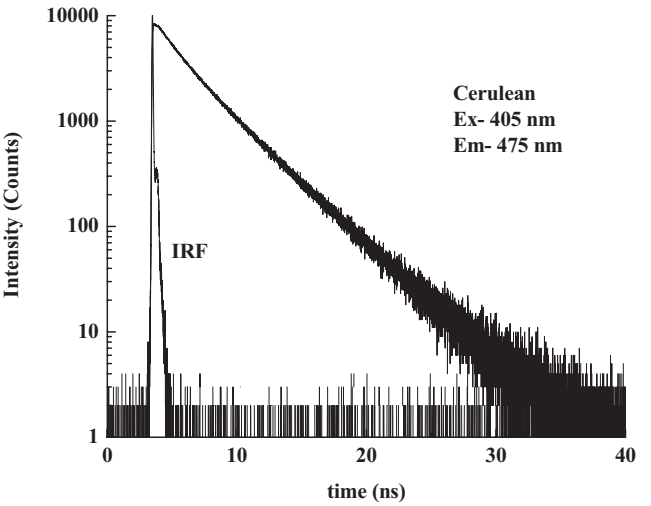

Fig. 5 Time-domain intensity decay of Cerulean. The decay is well approximated with a two exponential decay model (see Table 1). The amplitude and fractional intensity weighted average lifetimes are 2.82 and 3.23 ns respectively.

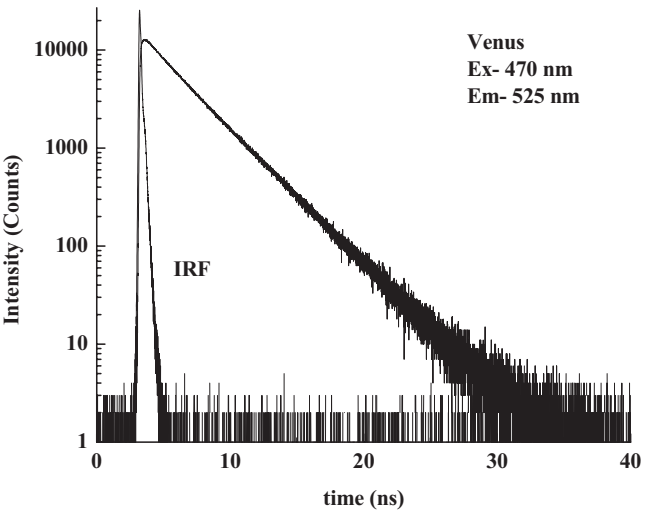

Fig. 6 Time-domain intensity decay of the Venus. The decay is well approximated using a two exponential decay model (see Table 1). The amplitude and fractional intensity weighted average lifetimes are 2.87 and 3.03 ns respectively.

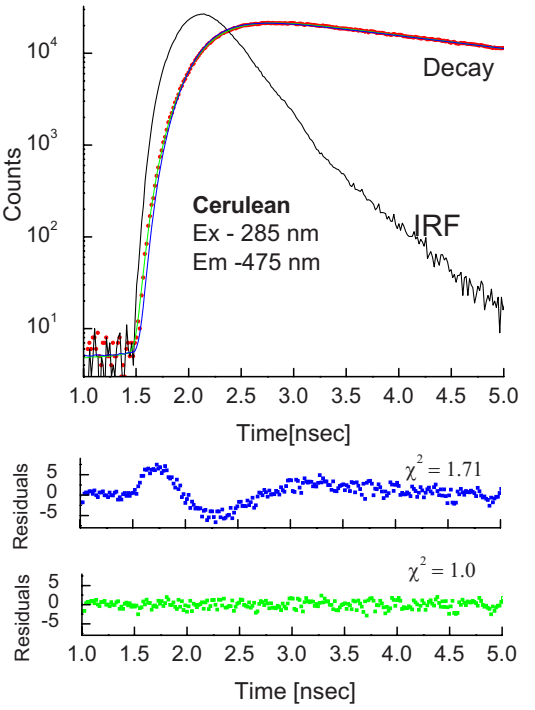

Fig. 7 Initial intensity decay of Cerulean with the excitation in Trp excitation region (285 nm). The blue line and residuals show the fit with positive component only, while the green line and residuals show the fit with one negative component. A negative component is needed to fit the data better. (Color online only.)

observed (Table 1). This is a characteristic property of a process occurring in the excited state. A negative component in the intensity decay indicates that the fluorescent protein chromophore is receiving additional "pumping" after excitation. This is consistent with FRET occurring between the aromatic amino acids and the fluorescent protein chromophore.

This is visualized in Figs. 7 and 8 for Cerulean and Venus respectively. Although the data were fitted for the whole decay, we present the fit only for the initial 5 ns, in order to show the necessity of negative component to fit the decay. The short decay time (0.16 and 0.2 ns for Cerulean and Venus, respectively) associated with the negative decay component shows that the energy transfer process is very efficient ($>90\%$) if we assume that the lifetime of unquenched tryptophan or tyrosine is $\sim$3 ns. This explains the absence of a significant tryptophan emission. The low steady-state excitation anisotropy value for Cerulean (Fig. 3) and negative value for Venus (Fig. 4) observed with excitation of $<$350 nm is consistent with significantly different near-orthogonal orientations for donor (Trp) and acceptor (fluorescent protein chromophore) transition moments. However, characterization of Trp donor profile was not an option due to presence of mild spectroscopic impurities (as seen in SDS-Page and Western Blot).

Anisotropy decays of both proteins (Figs. 9 and 10) are similar, displaying high values of initial anisotropy and corre-

Table 1 Multiexponential analysis of fluorescence intensity decays of Cerulean and Venus.

Protein	Ex (nm)	Em (nm)	α_1	T_1 (ns)	α_2	T_2 (ns)	α_3	T_3 (ns)	X^2
Cerulean	405	475	1.0	3.18±0.03	—	—	—	—	4.7
			0.403	1.52±0.04	0.597	3.70±0.02	—	—	0.9
	285	475	1.0	3.47±0.09	—	—	—	—	3.1
			0.936	2.08±0.03	1.253	4.02±0.02	−1.189	0.16±0.01	1.0
Venus	470	525	1.0	3.03±0.01	—	—	—	—	1.7
			0.160	1.31±0.07	0.840	3.17±0.01	—	—	0.9
	285	525	1.0	3.35±0.09	—	—	—	—	1.2
			1.835	3.31±0.02	−0.835	0.2±0.02	—	—	1.0

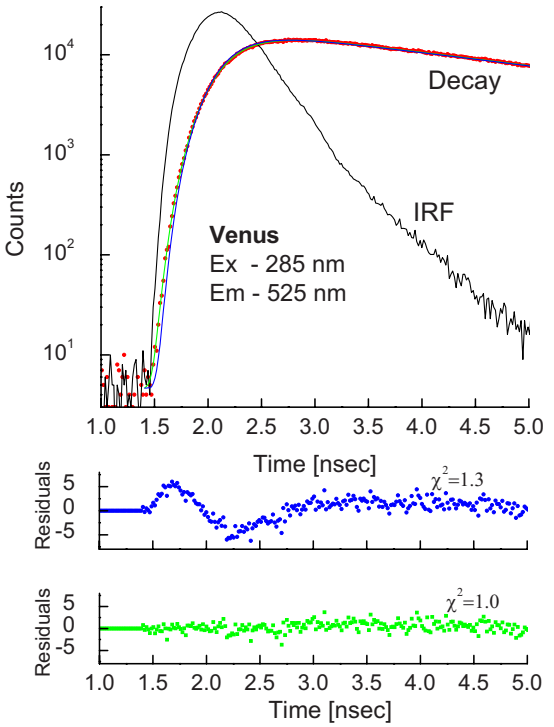

Fig. 8 The initial intensity decay of Venus with the excitation in Trp excitation region (285 nm). The blue colored line and residuals show the fit with positive component only, while green line and residuals show the fit with one negative component. A negative component is needed to fit the data better.

lation times of ~15 ns (Table 2). The fits to these decays can be modestly improved using a decay model with a second correlation time. However, these second correlation times are on the order of a few nanoseconds and are most likely associated with the nonspherical shape of the protein than with chromophore internal mobility. The very high steady-state anisotropies observed as well as the relatively slow anisotropy decays measured indicates that the fluorescent protein chromophores in Cerulean and Venus are rigidly oriented within the protein structure and have little freedom for rotation. This attribute should encourage polarization studies using fluorescent proteins, because the local fluorophore mobility is a bottleneck in many rotational diffusion investigations.

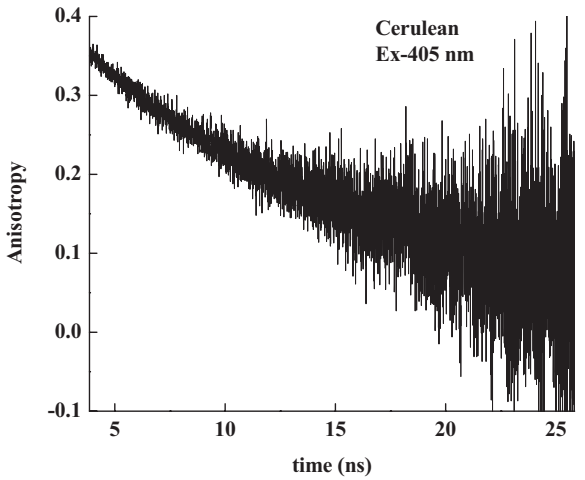

Fig. 9 Anisotropy decay of Cerulean. Two components are needed to fit the data well (See Table 2). The limiting anisotropy (r_0) was 0.4, and the rotational correlation times (θ_a and θ_b) were 6.7 and 19.6 ns.

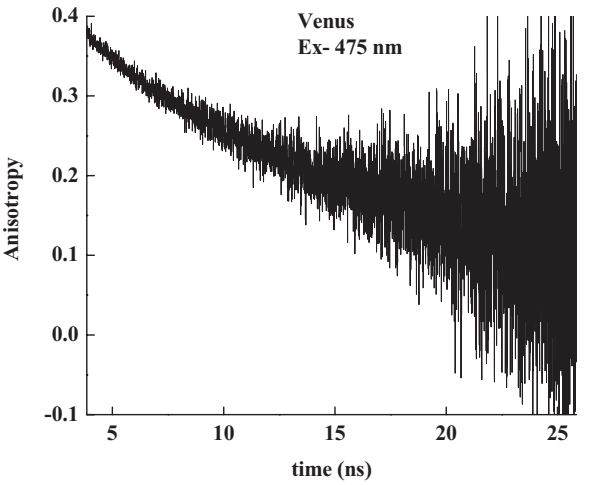

Fig. 10 Anisotropy decay of Venus. Two components are needed to fit the data well (See Table 2). The limiting anisotropy (r_0) was 0.4, and the rotational correlation times (θ_a and θ_b) were 3.7 and 20.3 ns.

3.3 *Fluorescence Quenching Study*

GFP fluorescence is known to be resistant to many quenching reagents. This is thought to arise from the GFP β-barrel protein structure that physically surrounds and sequester the GFP fluorophore from water soluble factors.[25,26] We next wanted to determine if the β-barrel structure of Cerulean and Venus would also protect their fluorophores from quenching reagents. We also wanted to determine if the high-efficiency energy transfer observed with UV excitation was also insensitive to external quenchers. First, we noted that with long-wavelength excitations, even high concentrations of acrylamide or potassium iodide (KI) in the solution do not change the emissions of Cereluan or Venus proteins (data not shown). This indicates that their chromophores are not readily accessible to these quenchers.

Next, we used UV excitation to test if the tryptophan fluorophore is also protected by the β-barrel structure. Figures 11 and 12 show the effect of acrylamide and/or KI presence on the UV-excited Cereluan and Venus proteins. There was little evidence for quenching of either Cerulean or Venus fluorescence. We conclude that the fluorescent protein chromophores as well as the tryptophan residue is effectively shielded from these quenchers. One can note that, in the presence of acrylamide, the emission spectrum of our purified Cerulean (and to a lesser extent Venus) was reduced at 400–450 nm (Fig. 11). Presumably, tryptophan in a small fraction of denatured fluorescent proteins can be quenched.

We decided to test if the unique protective nature of the fluorescent protein β-barrel structure can be exploited to suppress background fluorescence in fluorescent protein experiments. We prepared the mixture of Cereluan or Venus proteins with flavin mononucleotide (FMN). Flavins are an abundant chemical moiety found in cells. A major obstacle to live-cell

Table 2 Anisotropy decay analyses of Cerulean and Venus emission.

Protein	r_1	θ_1 (ns)	r_2	θ_2 (ns)	$\bar{\theta}$ (ns)	X_r^2
Cerulean	0.352±0.002	14.5±0.5	—	—	14.5	1.6
	0.088±0.001	6.7±0.4	0.266±0.002	19.6±0.6	18.3	1.5
Venus	0.374±0.002	16.4±0.6	—	—	16.4	2.0
	0.048±0.001	3.7±0.4	0.331±0.002	21.4±0.7	20.3	1.8

florescence imaging is that flavin fluorescence often masks the fluorescence of less abundant exogenous fluorophores experimentally introduced into cells. To illustrate this, a solution of either Cerulean (Fig. 13) or Venus (Fig. 14) and the flavin FMN were prepared and their emission spectra recorded. As expected, the strong FMN emission masked the fluorescent protein spectra in these mixtures. Addition of 0.35 Molar KI selectively quenched FMN to reveal the previously masked fluorescence protein spectra. To illustrate this effect, we prepared and imaged a microscopy slide with immobilized Venus protein (Fig. 15, star-shaped spot). Next, a drop of FMN solution was applied to the slide, primarily over the immobilized Venus. This led to fluorescence dominated by FMN. The star-shaped Venus spot could not be distinguished. Finally, we progressively added KI solution [Fig. 15(b)]. As FMN was selectively quenched, the fluorescent Venus protein spot was again revealed.

4 Conclusions

In addition to excitation with visible light (400–550 nm) both, Cereluan and Venus fluorescent proteins can be efficiently excited in the UV region at wavelengths (280 nm), where tryptophan and tyrosine are excited. Surprisingly, appreciable emission from these aromatic amino acids was not observed in the emission spectra of fluorescent proteins when excited with UV light (285 nm). UV excitation is thought to be accompanied by a very efficient energy transfer from aromatic amino acids (presumably tryptophan and/or tyrosine) to the fluorescent protein chromophore because, under these conditions, a negative lifetime decay component (pumping) was observed in the fluorescence intensity decay. The lifetime associated with this lifetime decay component was <200 ps. Assuming a nonquenched lifetime of tryptophan/tyrosine species of ~ 3 ns, one can calculate a transfer efficiency of $>90\%$. With such a high-energy-transfer efficiency, it is not surprising that the fluorescence spectra of tryptophan in fluorescent proteins cannot be measured accurately. Also, presence of trace amount of impurities in the sample (Fig. 1) contribute to the signal seen at the Trp emission region, mak-

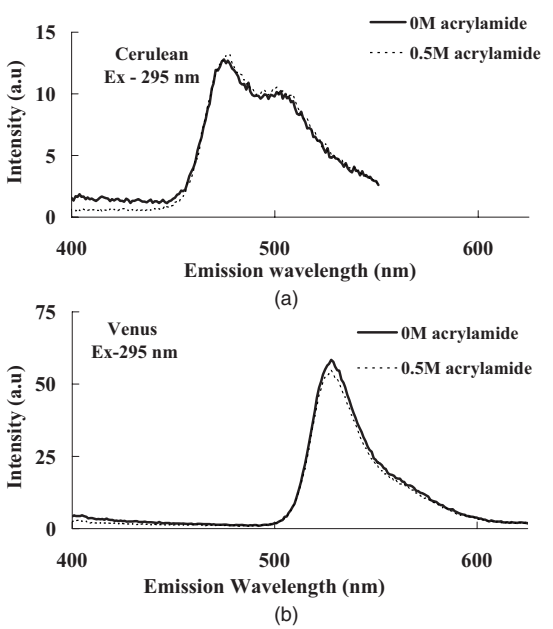

Fig. 11 Effect of acrylamide on (a) the fluorescence of Cerulean and (b) Venus.

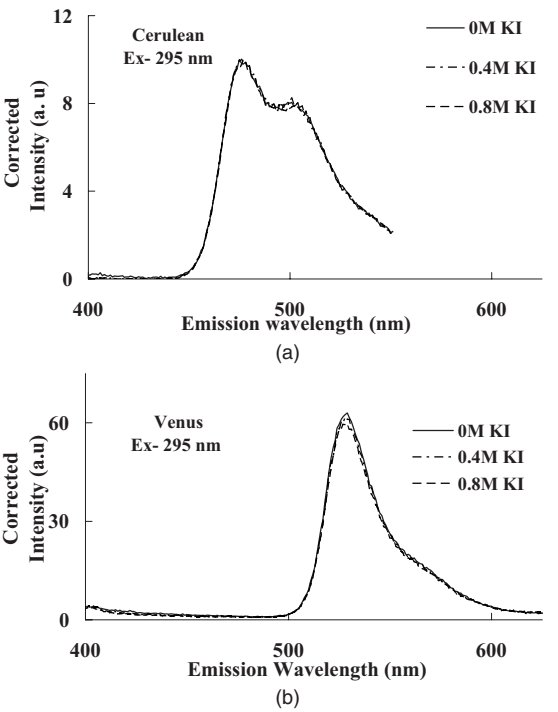

Fig. 12 Effect of KI on the (a) fluorescence spectrum of Cerulean and (b) Venus.

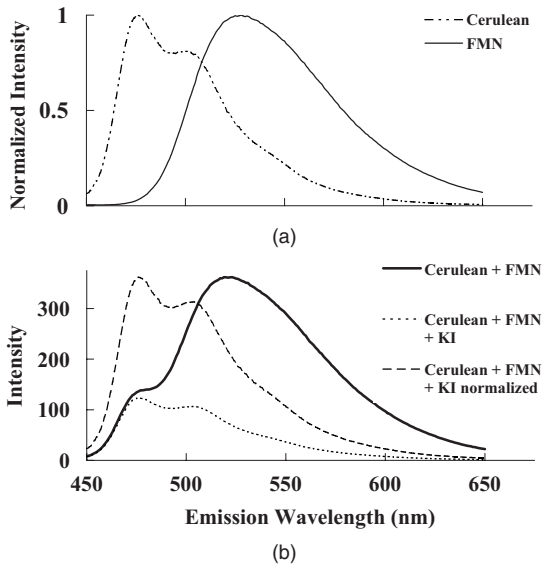

Fig. 13 Effect of KI on the fluorescence mixture of Cerulean and FMN. (a) Normalized emission spectra of Cerulean and FMN. (b) Emission spectrum of mixture in absence (solid thick lines) and presence (dotted lines) of KI. Dashed line represent normalized spectrum of mixture in presence of KI.

ing the interpretation even more complex. Furthermore, steady-state anisotropy measurements of the Cerulean or Venus fluorophore were only low with UV excitation, again indicating energy transfer between an aromatic amino acid and the fluorescent protein chromophore.

Time-resolved fluorescence anisotropy decay analysis also revealed that the emission dipole orientation of the Cereluan and Venus chromophores are rigidly fixed in the protein structure. This conclusion is based on our inability to detect any local, subnanosecond decay component in time-resolved an-

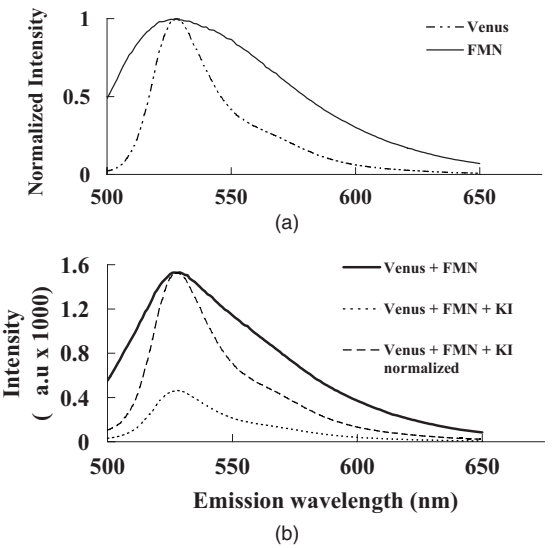

Fig. 14 Effect of KI on the fluorescence mixture of Venus and FMN. (a) Normalized emission spectra of Venus and FMN. (b) Emission spectrum of mixture in absence (solid thick lines) and presence (dotted lines) of KI. Dashed line represent normalized spectrum of mixture in presence of KI.

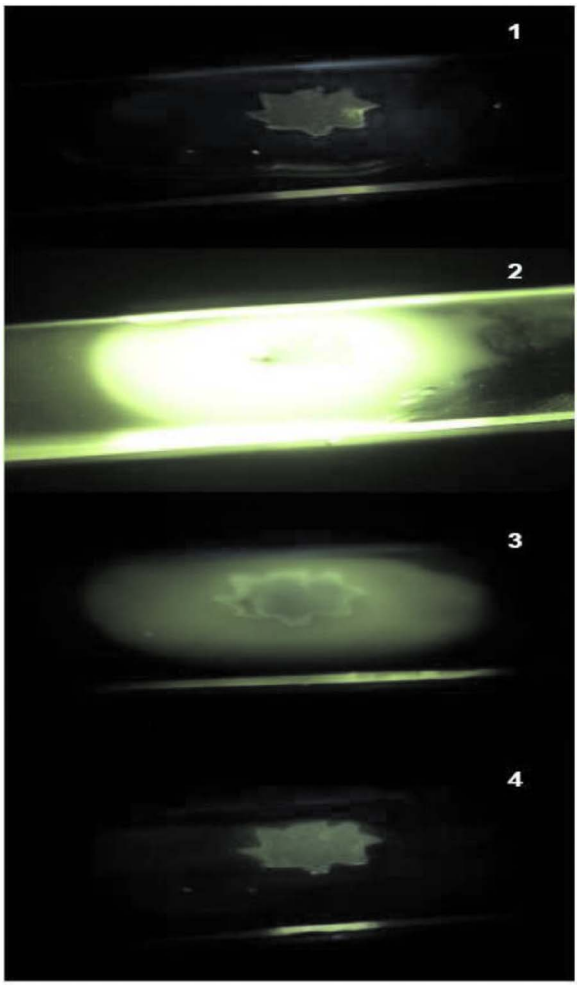

Fig. 15 Photograph of the combination of Venus and FMN emissions. Venus is immobilized at the surface of the glass slide (1). Next the slide was flooded with 500 μM FMN solution (2). Then solution of 2M KI was added drop wise; 2–3 drops (3 and 4). The illumination was from 450 nm LED, Observation was through 495 LWP filter. Canon® EOS 300D camera with an 18–35 mm lens was used to take the photograph using a shutter speed of 3 min. Images were trimmed by Canon ZoomBrowser® software. No additional modifications were made with the photographs.

isotropy measurements. The presence of trace impurities in the sample makes the interpretation of fluorescence decay from the internal tryptophan more complex. This prevented us from determining if the orientation of its emission dipole is also rigidly fixed. Nonetheless, the negative steady-state anisotropy observed with UV excitation of Venus, which contains only one tryptophan residue, strongly indicates energy transfer from tryptophan residues to the chromophore region. The excitation anisotropy (while acceptor emission was observed) value dropped for Cerulean, but still remained positive. This can be due to presence of two tryptophan residues in Cerulean.

Both, tryptophan and the fluorescent protein chromophore are buried in the protein structure and not accessible to the external quenchers, acrylamide and/or KI. This is a unique advantage of fluorescent proteins over other probes. We have shown that quenchers can be used to selectively suppress non-

specific fluorescent background. In biological samples, such as cells or tissue, fluorescent background is a major obstacle in any fluorescence study, especially in those based on FRET. Our observation that the fluorescence of purified Venus is selectively spared while the fluorescence of FMN is almost completely quenched suggests that using KI solution in washing procedures will improve the ratio of fluorescent protein emission to background fluorescence. We understand that high concentrations of iodide will be toxic to the cell itself and thus cannot be used in live-cell imaging instantaneously. But this study proves the concept that using flavin quenchers can be a good strategy of improving signal-to-noise ratio in imaging experiments that use these fluorescent proteins. Use of other known quenchers of flavin, such as oxygen or reducing flavins in the cells, can be a potentially feasible future strategy. These simple experimental manipulations might be the key for allowing quantitative imaging of fluorescent proteins in cells with high background fluorescence (such as neurons) or for readily detecting the fluorescence emission of single fluorescent protein molecules by dramatically increasing the signal-to-noise ratio.

Acknowledgments

This research was supported by the National Institutes of Health Project No. ZO1AA000452-01 to S.S.V., and by the Texas Emerging Technologies Fund Grant to Z. G.

References

1. J. Lippincott-Schwartz, E. Snapp, and A. Kenworthy, "Studying protein dynamics in living cells," *Nat. Rev. Mol. Cell Biol.* **2**(6), 444–456 (2001).
2. J. Zhang, R. E. Campbell, A. Y. Ting, and R. Y. Tsien, "Creating new fluorescent probes for cell biology," *Nat. Rev. Mol. Cell Biol.* **3**(12), 906–918 (2002).
3. A. Crameri, E. A. Whitehorn, E. Tate, and W. P. Stemmer, "Improved green fluorescent protein by molecular evolution using DNA shuffling," *Nat. Biotechnol.* **14**(3), 315–319 (1996).
4. R. Heim, D. C. Prasher, and R. Y. Tsien, "Wavelength mutations and posttranslational autoxidation of green fluorescent protein," *Proc. Natl. Acad. Sci. U.S.A.* **91**(26), 12501–12504 (1994).
5. L. S. Barak, S. S. Ferguson, J. Zhang, C. Martenson, T. Meyer, and M. G. Caron, "Internal trafficking and surface mobility of a functionally intact beta2-adrenergic receptor-green fluorescent protein conjugate," *Mol. Pharmacol.* **51**(2), 177–184 (1997).
6. S. P. Dobson, C. Livingstone, G. W. Gould, and J. M. Tavare, "Dynamics of insulin-stimulated translocation of GLUT4 in single living cells visualised using green fluorescent protein," *FEBS Lett.* **393**(2–3), 179–184 (1996).
7. T. Nakamura, K. Aoki, and M. Matsuda, "Monitoring spatio-temporal regulation of Ras and Rho GTPase with GFP-based FRET probes," *Methods* **37**(2), 146–153 (2005).
8. M. L. Nonet, "Visualization of synaptic specializations in live *C. elegans* with synaptic vesicle protein-GFP fusions," *J. Neurosci. Methods* **89**(1), 33–40 (1999).
9. D. Toomre, P. Keller, J. White, J. C. Olivo, and K. Simons, "Dual-color visualization of trans-Golgi network to plasma membrane traffic along microtubules in living cells," *J. Cell. Sci.* **112**(Pt 1), 21–33 (1999).
10. N. C. Shaner, P. A. Steinbach, and R. Y. Tsien, "A guide to choosing fluorescent proteins," *Nat. Methods* **2**(12), 905–909 (2005).
11. M. M. Falk and U. Lauf, "High resolution, fluorescence deconvolution microscopy and tagging with the autofluorescent tracers CFP, GFP, and YFP to study the structural composition of gap junctions in living cells," *Microsc. Res. Tech.* **52**(3), 251–262 (2001).
12. C. Thaler, S. V. Koushik, P. S. Blank, and S. S. Vogel, "Quantitative multiphoton spectral imaging and its use for measuring resonance energy transfer," *Biophys. J.* **89**(4), 2736–2749 (2005).
13. Y. Chen, J. D. Mills, and A. Periasamy, "Protein localization in living cells and tissues using FRET and FLIM," *Differentiation* **71**(9–10), 528–541 (2003).
14. A. G. Harpur, F. S. Wouters, and P. I. Bastiaens, "Imaging FRET between spectrally similar GFP molecules in single cells," *Nat. Biotechnol.* **19**(2), 167–169 (2001).
15. F. S. Wouters and P. I. Bastiaens, "Fluorescence lifetime imaging of receptor tyrosine kinase activity in cells," *Curr. Biol.* **9**(19), 1127–1130 (1999).
16. A. H. Clayton, Q. S. Hanley, D. J. Arndt-Jovin, V. Subramaniam, and T. M. Jovin, "Dynamic fluorescence anisotropy imaging microscopy in the frequency domain (rFLIM)," *Biophys. J.* **83**(3), 1631–1649 (2002).
17. I. Gautier, "Homo-FRET microscopy in living cells to measure monomer-dimer transition of GFP-tagged proteins," *Biophys. J.* **80**(6), 3000–3008 (2001).
18. D. S. Lidke, "Imaging molecular interactions in cells by dynamic and static fluorescence anisotropy (rFLIM and emFRET)," *Biochem. Soc. Trans.* **31**(Pt 5), 1020–1027 (2003).
19. L. W. Runnels and S. F. Scarlata, "Theory and application of fluorescence homotransfer to melittin oligomerization," *Biophys. J.* **69**(4), 1569–1583 (1995).
20. D. M. Jameson, J. C. Croney, and P. D. Moens, "Fluorescence: basic concepts, practical aspects, and some anecdotes," *Methods Enzymol.* **360**, 1–43 (2003).
21. J. R. Lakowicz, *Principles of Fluorescence Spectroscopy*, Wiley-VCH, Weinheim (1999).
22. B. Valeur, *Molecular Fluorescence*, Plenum, New York (2002).
23. M. A. Rizzo, G. H. Springer, B. Granada, and D. W. Piston, "An improved cyan fluorescent protein variant useful for FRET," *Nat. Biotechnol.* **22**(4), 445–449 (2004).
24. T. Nagai, K. Ibata, E. S. Park, M. Kubota, K. Mikoshiba, and A. Miyawaki, "A variant of yellow fluorescent protein with fast and efficient maturation for cell-biological applications," *Nat. Biotechnol.* **20**(1), 87–90 (2002).
25. A. Rekas, J. R. Alattia, T. Nagai, A. Miyawaki, and M. Ikura, "Crystal structure of venus, a yellow fluorescent protein with improved maturation and reduced environmental sensitivity," *J. Biol. Chem.* **277**(52), 50573–50578 (2002).
26. G. D. Malo, "X-ray structure of Cerulean GFP: a tryptophan-based chromophore useful for fluorescence lifetime imaging," *Biochemistry* **46**(35), 9865–9873 (2007).
27. S. T. Hess, E. D. Sheets, A. Wagenknecht-Wiesner, and A. A. Heikal, "Quantitative analysis of the fluorescence properties of intrinsically fluorescent proteins in living cells," *Biophys. J.* **85**(4), 2566–2580 (2003).
28. S. Inoue, O. Shimomura, M. Goda, M. Shribak, and P. T. Tran, "Fluorescence polarization of green fluorescence protein," *Proc. Natl. Acad. Sci. U.S.A.* **99**(7), 4272–4277 (2002).
29. G. H. Patterson, S. M. Knobel, W. D. Sharif, S. R. Kain, and D. W. Piston, "Use of the green fluorescent protein and its mutants in quantitative fluorescence microscopy," *Biophys. J.* **73**(5), 2782–2790 (1997).
30. K. Suhling, "Imaging the environment of green fluorescent protein," *Biophys. J.* **83**(6), 3589–3595 (2002).
31. A. F. Bell, D. Stoner-Ma, R. M. Wachter, and P. J. Tonge, "Light-driven decarboxylation of wild-type green fluorescent protein," *J. Am. Chem. Soc.* **125**(23), 6919–6926 (2003).
32. J. J. van Thor, A. J. Pierik, I. Nugteren-Roodzant, A. Xie, and K. J. Hellingwerf, "Characterization of the photoconversion of green fluorescent protein with FTIR spectroscopy," *Biochemistry* **37**(48), 16915–16921 (1998).
33. A. Volkmer, V. Subramaniam, D. J. Birch, and T. M. Jovin, "One- and two-photon excited fluorescence lifetimes and anisotropy decays of green fluorescent proteins," *Biophys. J.* **78**(3), 1589–1598 (2000).